

## Self-Assembly of Phospholipid Molecules at a Au(111) Electrode Surface

Shimin Xu, Grzegorz Szymanski, and Jacek Lipkowski\*

Department of Chemistry and Biochemistry, University of Guelph, Guelph, Ontario, Canada, N1G 2W1

Received July 19, 2004; E-mail: lipkowski@chembio.uoguelph.ca

Phospholipid bilayers formed by fusion of small unilamellar vesicles (SUVs) onto glass, mica, or organic-modified surfaces constitute an attractive model of a biological membrane for studying membrane processes.<sup>1</sup> Monolayers<sup>2</sup> and bilayers<sup>2b,3</sup> of phospholipids may also be deposited or tethered to surfaces of metal electrodes such as mercury or gold, which can then be used to study the influence of electric field on voltage-gated membrane proteins and lipid–lipid and lipid–protein interactions.<sup>4</sup> Therefore, significant efforts have been made to study the mechanism by which phospholipids spread at solid supports.<sup>5</sup> The objective of this note is to describe the first electrochemical scanning tunneling microscopy (EC-STM) studies of spreading 1,2-dimyristoyl-sn-glycero-3-phosphatidylcholine (DMPC) vesicles into a film at a Au(111) electrode surface. We will show that during the initial stage, DMPC molecules adsorb flat with the acyl chains oriented parallel to the surface and assemble into an ordered monolayer similar to the monolayer formed by alkanes.<sup>6</sup> With time, the molecules reorient and the monolayer is transformed into a hemimicellar film.

The experiments were carried out in a dilute aqueous solution of SUVs  $\sim 4 \times 10^{-5}$  M total DMPC (Sigma, 99.0+%, St. Louis, MO) concentration in 50 mM KClO<sub>4</sub> (ACS Certified Fisher, Fair Lawn, NJ, twice recrystallized). All images were acquired with a Nanoscope II EC-STM (Digital Instrument, Santa Barbara, CA) with an A scanner using a constant-current mode. A small bead produced by melting a gold wire spot welded to a gold plate was the working electrode. The (111) facets at the bead surface were used for the acquisition of images. The electrode was flame annealed before each experiment. A gold ring was the counter electrode, and a miniaturized Ag/AgCl (saturated KCl) was the reference electrode ( $-40$  mV vs the saturated calomel electrode). The STM tips were electrochemically etched tungsten wires coated with transparent polyethylene. All images were acquired at a potential of  $E = 200$  mV (Ag/AgCl) at which the charge density at the Au(111) surface was close to zero.

Figure 1 shows an image of the Au(111) surface acquired 3 min after injection of a dilute solution of DMPC vesicles into the electrochemical cell of the STM instrument. The image reveals rows formed by DMPC molecules crossing the double lines of the substrate, which are characteristic of a reconstructed Au(111) surface.<sup>7</sup> The adsorbed layer consists of several domains that are rotated by 60° or 120°. The molecular rows are oriented at an angle of 60° (on other images the angle varied between 50 and 70°) with respect to the direction of the reconstruction lines of the underlying gold surface. A change of the direction of the reconstruction line by 120° has no effect on the ordering of the DMPC molecules. However, the domain boundaries of the organic adlayer coincide with the surface reconstruction domain boundaries. The average width of the molecular row, measured as a valley to valley distance in the direction normal to the row, amounts to  $4.4 \pm 0.2$  nm. The separation between the reconstruction line is equal to 6.3 nm, consistent with the literature.<sup>7</sup>

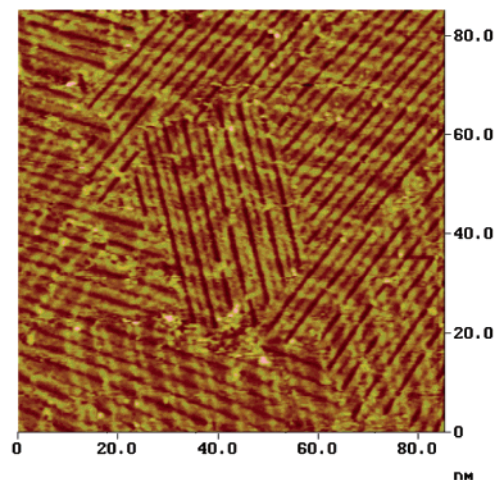


**Figure 1.** Image of a Au (111) surface at  $E = +200$  mV acquired 3 min after injection of a solution of DMPC vesicles (0.04 M total DMPC concentration). Supporting electrolyte: 50 mM KClO<sub>4</sub>. Imaging conditions:  $I_t = 729.0$  pA,  $E_{tip} = -150$  mV.

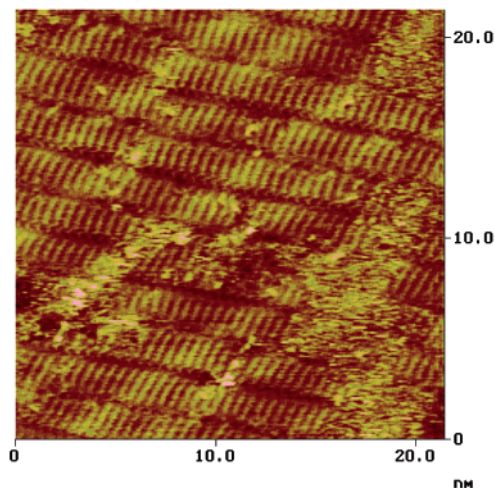


**Figure 2.** Higher resolution image of the monolayer of DMPC on Au (111) at +200 mV in 50 mM KClO<sub>4</sub> with 0.04 M total DMPC concentration. Imaging conditions:  $I_t = 1.00$  nA,  $E_{tip} = -150$  mV.

Figure 2 shows a higher resolution image of the DMPC adlayer. It reveals that each row consists of two parallel bands of closely packed molecules ( $\sim 2$  nm long stripes) separated by a distance  $0.50 \pm 0.02$  nm in the direction normal to the molecular axis. The molecular axes are always oriented at 30° with respect to the direction of the reconstruction line. The angle between the molecular axes and the direction of the molecular row may vary within the range of  $90 \pm 10^\circ$ . This gives a spread of the angles between the molecular row and the reconstruction line within the limits  $60 \pm 10^\circ$ .

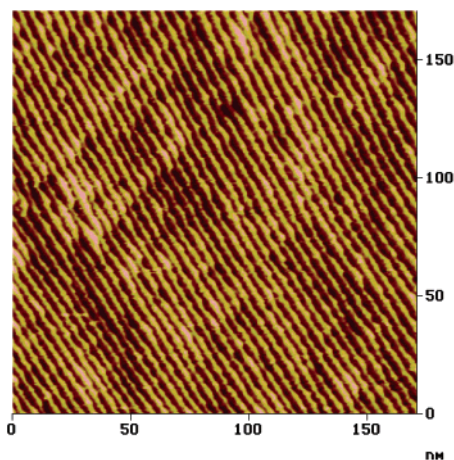


**Figure 3.** Hemimicellar structure of a film of DMPC molecules at a Au(111) electrode at +200 mV in 50 mM KClO<sub>4</sub> with 0.04 M total DMPC concentration. Imaging conditions:  $I_t = 1.00$  nA,  $E_{tip} = -150$  mV.

These properties indicate that packing of DMPC molecules into a two-dimensional, ordered adlayer is quite similar to the packing of *n*-alkanes at the Au(111) surface.<sup>6</sup> The  $0.50 \pm 0.02$  nm distance between molecular stripes is equal to the distance between two alkyl chains in an ordered adlayer of alkanes.<sup>6</sup> Apparently, the stripes are images of individual acyl chains of the DMPC molecule. Like alkanes, the phospholipid molecules are assembled by aligning the acyl chains in the nearest neighbor direction NN (the [011] direction) of the reconstructed Au(111) surface. This behavior indicates that ordering of DMPC molecules is to a large extent determined by chain–substrate interactions. The chain–chain and polar head–polar head interactions control the angle between the molecular axis and the row direction and this in turn determines the angle between the row and the reconstruction line. The molecular rows form a 60° angle with the reconstruction line when the molecular axes are normal to the row direction. When the molecular axes are oriented at 80° with respect to the row, the angle between the row and the reconstruction line is 50 or 70°.

The thickness of the DMPC bilayer in a single crystal of DMPC, determined by X-ray diffraction, is equal to 5.49 nm, with 3.4 nm corresponding to the hydrocarbon region and 2.09 nm to the polar head region.<sup>8</sup> The thickness of two molecular rows that constitute the repeat unit in the STM images is about 1 nm smaller. This behavior suggests that the polar heads are rotated out of the plane of the two acyl chains and directed toward the solution. This conformation allows the head to remain in a fully hydrated state.

The images show stripes of the acyl chains, but the polar head region of the DMPC is invisible. The ability to image an insulating molecule by STM may be explained in terms of a weak coupling between electronic states in the adsorbate and in the substrate near the Fermi level that gives the adsorbate a property of an antenna capable of receiving tunneling electrons.<sup>6e,9</sup> Therefore, the coupling for the polar head region is poor or the polar head is mobile. The two acyl chains are connected through the ester bonds to the glycerol moiety. Indeed, images of “U”-shaped features could be seen in Figure 2 and other high-resolution images not shown here. However, the contrast (coupling) is weaker for the glycerol moiety of the molecule than for the acyl chains.

The images of flat-lying DMPC molecules could be observed only in dilute vesicle solutions and during a short period of time after the injection of vesicles to the cell. After about 30 min, the film was transformed into a totally different structure, as shown in

Figure 3. The Au(111) surface is covered by long stripes 4.5 nm wide with a 0.13 nm peak to valley corrugation and a thickness of  $2.2 \pm 0.1$  nm, determined from an independently measured force distance curve using an atomic force microscopy (AFM) instrument. The thickness of the film is slightly less than one monolayer, and the molecular resolution is lost. This structure is characteristic for the aggregation of zwitterionic and ionic surfactants into a hemimicellar state in which the long rows represent hemicylindrical surface micelles.<sup>10</sup>

At hydrophilic surfaces such as glass, quartz, and mica, spreading of vesicles involves adsorption, rupture, and either sliding of a single bilayer or rolling of two juxtaposed bilayers in a tank tread-type motion<sup>1,5</sup> on a thin lubricating film of the solvent. In this note we present the first evidence that spreading of phospholipids from vesicles at a gold electrode surface involves a different mechanism. The molecules released by rupture of a vesicle initially self-assemble at the metal surface into a well-ordered monolayer. The self-assembly is controlled by the acyl chain–metal surface interaction. When more molecules accumulate at the surface, the monolayer is transformed into a hemimicellar state. In solutions with high vesicle concentrations, the hemimicellar state is transformed further into a bilayer.<sup>3c–e</sup>

**Acknowledgment.** This work has been supported by the Natural Sciences and Engineering Research Council of Canada (NSERC). J.L. acknowledges CFI for the Canada Research Chair Award.

## References

- (1) (a) Sackmann, E. *Science* **1996**, *271*, 43. (b) Xie, A. F.; Yamada, R.; Gewirth, A. A.; Garnick, S. *Phys. Rev. Lett.* **2002**, *89*, 246103. (c) Leonenko, Z. V.; Carnini, A.; Cramb, D. T. *Biochim. Biophys. Acta* **2000**, *1509*, 131.
- (2) (a) Bizzotto, D.; Nelson, A. *Langmuir* **1998**, *14*, 6269. (b) Prieto, F.; Navarro, I.; Rueda, M. J. *Electroanal. Chem.* **2003**, *550*, 253. (c) Moncelli, M. R.; Becucci, L.; Nelson, A.; Guidelli, R. *Biophys. J.* **1996**, *70*, 2716. (d) Nelson, A.; Bizzotto, D. *Langmuir* **1999**, *15*, 7031. (e) Guidelli, R.; Aloisi, G.; Becucci, L.; Dolfi, A.; Moncelli, M. R.; Buoninsegni, F. T. *J. Electroanal. Chem.* **2001**, *504*, 1.
- (3) (a) Stauffer, V.; Stoodly, R.; Agak, J. O.; Bizzotto, D. *J. Electroanal. Chem.* **2001**, *516*, 73. (b) Hepel, M. *J. Electroanal. Chem.* **2001**, *509*, 90. (c) Horswell, S. L.; Zamlynnny, V.; Li, H.-Q.; Merrill, A. R.; Lipkowski, J. *Faraday Discuss.* **2002**, *121*, 405. (d) Zawisza, I.; Lachenwitzer, A.; Zamlynnny, V.; Horswell, S. L.; Goddard, J. D.; Lipkowski, J. *Biophys. J.* **2003**, *85*, 4055. (e) Burgess, I.; Li, M.; Horswell, S. L.; Szymanski G.; Lipkowski, J.; Majewski, J.; Satija, S. *Biophys. J.* **2004**, *86*, 1763.
- (4) (a) Jones, S. W. *J. Bioenerg. Biomembr.* **1998**, *30*, 299. (b) Terlau, H.; Stuhmer, W. *Naturwissenschaften* **1998**, *85*, 437. (c) Olivotto, M.; Arcangeli, A.; Carla, M.; Wanke, E. *Bioessays* **1996**, *18*, 495.
- (5) (a) Raedler, J.; Strey, H.; Sackmann, E. *Langmuir* **1995**, *11*, 4539. (b) Keller, C. A.; Kasemo, B. *Biophys. J.* **1998**, *75*, 1397. (c) Seifert, U. *Adv. Phys.* **1997**, *46*, 13. (d) Lipowsky, R.; Seifert, U. *Mol. Cryst. Liq. Cryst.* **1991**, *202*, 17. (e) Zhdanov, V. P.; Kasemo, B. *Langmuir* **2001**, *17*, 3518. (f) Reviakine, I.; Brisson, A. *Langmuir* **2000**, *16*, 1806.
- (6) (a) Uosaki, K.; Yamada, R. *J. Am. Chem. Soc.* **1999**, *121*, 4090. (b) Yamada, R.; Uosaki, K. *J. Phys. Chem. B* **2000**, *104*, 6021. (c) Marchenko, O.; Cousty, J. *Phys. Rev. Lett.* **2000**, *84*, 5363. (d) Marchenko, A.; Cousty, J.; Van, L. P. *Langmuir* **2002**, *18*, 1171. (e) He, Y.; Ye, T.; Borguet, E. *J. Phys. Chem. B* **2002**, *106*, 1264. (f) Xie, Z. X.; Xu, X.; Tang, J.; Mao, B. W. *J. Phys. Chem. B* **2000**, *104*, 11719. (g) Xie, Z. X.; Huang, Z. F.; Xu, X. *Phys. Chem. Chem. Phys.* **2002**, *4*, 1486. (h) Zhang, H. M.; Xie, Z. X.; Mao, B. W.; Xu, X. *Chem. Eur. J.* **2004**, *10*, 1415.
- (7) (a) Kolb, D. M. *Prog. Surf. Sci.* **1996**, *51*, 109. (b) Gao, X.; Hamelin, A.; Weaver, M. J. *Phys. Chem.* **1991**, *95*, 6993.
- (8) (a) Pearson, R. H.; Pascher, I. *Nature* **1979**, *281*, 499. (b) Hauser, H.; Pascher, I.; Pearson, R. H.; Sundell, S. *Biochim. Biophys. Acta* **1981**, *650*, 21.
- (9) Giancarlo, L. C.; Flynn, G. W. *Annu. Rev. Phys. Chem.* **1998**, *49*, 297.
- (10) (a) Manne, S.; Gaub, H. E. *Science* **1995**, *270*, 1480. (b) Jaschke, M.; Butt, H.-J.; Gaub, H. E.; Manne, S. *Langmuir* **1997**, *13*, 1381. (c) Liu, J.-F.; Min, G.; Ducker, W. A. *Langmuir* **2001**, *17*, 4895. (d) Burgess, I.; Jeffrey, C. A.; Cai, X.; Szymanski, G.; Galus, Z.; Lipkowski, J. *Langmuir* **1999**, *15*, 2607. (e) Burgess, I.; Zamlynnny, V.; Szymanski, G.; Lipkowski, J.; Majewski, J.; Smith, G.; Satija, S.; Ivkov, R. *Langmuir* **2001**, *17*, 3355. (f) Petri, M.; Kolb, D. M. *Phys. Chem. Chem. Phys.* **2002**, *4*, 1211.

JA045669A